SCIENTIFIC Publishing Limited

Trends in Immunotherapy

https://ojs.ukscip.com/index.php/ti

Article

Circulating MicroRNAs and Immune-Associated Pathways in Parkinson's Disease and Cutaneous Melanoma: An Integrative Analysis

Ana Lucia Ekowati [1], Hendra Pramono [2], Andrea Aprilia [3] and Ferbian Milas Siswanto [4,*]

[1] Department of Medical Biology, School of Medicine and Health Sciences, Atma Jaya Catholic University of Indonesia, Jakarta 14440, Indonesia; ana.lucia@atmajaya.ac.id

[2] Undergraduate Program, School of Medicine and Health Sciences, Atma Jaya Catholic University of Indonesia, Jakarta 14440, Indonesia; hendra.202206000018@student.atmajaya.ac.id

[3] Clinical Pathology Department, School of Medicine and Health Sciences, Atma Jaya Catholic University of Indonesia, Jakarta 14440, Indonesia; andrea.aprilia@atmajaya.ac.id

[4] Department of Biochemistry, School of Medicine and Health Sciences, Atma Jaya Catholic University of Indonesia, Jakarta 14440, Indonesia

[*] Correspondence: ferbian.siswanto@atmajaya.ac.id

Received: 2 October 2026; **Revised:** 19 October 2026; **Accepted:** 11 November 2026; **Published:** 24 November 2026

Abstract: Parkinson's disease (PD) and cutaneous melanoma are epidemiologically associated, but shared immune signatures cannot establish the cause of their co-occurrence. This hypothesis-generating integrative study used publicly available Parkinson's disease (PD) and cutaneous melanoma data to examine circulating miRNA associations and overlapping immune-expression contexts; it was not designed to establish a shared mechanism or explain the epidemiological co-occurrence of the two diseases. We integrated publicly available circulating and extracellular-vesicle (EV) microRNA (miRNA) evidence, independently reanalyzed PD serum counts with DESeq2, reviewed published pathway and single-cell findings, and calculated sample-level TCGA-SKCM (The Cancer Genome Atlas–Skin Cutaneous Melanoma) immune-expression associations with adjustment for tumor purity and leukocyte-associated expression. The site-matched PD serum analysis identified 26 FDR-significant miRNAs. miR-215-5p showed relatively consistent decreases across PD cohorts, whereas miR-574-5p and miR-584-5p were strongly heterogeneous across EV cohorts. Melanoma miR-574-5p disease-associated plasma findings and miR-215-5p EV evidence differed in independence and orthogonal validation. Literature-derived pathway studies identified partially overlapping inflammatory contexts. In TCGA-SKCM, most unadjusted TLR8 correlations with immune modules were attenuated after joint adjustment for consensus tumor purity, pan-leukocyte expression, and sample type; a residual IFNγ-response association (partial $\rho = 0.252$; bootstrap 95% CI 0.167–0.357) and weaker myeloid association ($\rho = 0.208$; 95% CI 0.096–0.325) persisted. Source auditing confirmed direct experimental support for a subset of nominated canonical miRNA targets. Critically, the strongest mechanistic evidence that extracellular miR-574-5p can engage human TLR8 derives from experimental systems in other diseases, not from the PD or melanoma patient samples analyzed here; the present data therefore do not demonstrate miR-574-5p–TLR8 signaling in either disease. These observations generate a specific, falsifiable extracellular miRNA–TLR8 hypothesis for direct experimental testing rather than establishing an inter-disease mechanism.

Keywords: Cutaneous Melanoma; MicroRNA; Parkinson's Disease; TLR8; Tumor Immunity

1. Introduction

Parkinson's disease (PD) and cutaneous melanoma (CM) represent distinct pathological conditions, but the epidemiological evidence shows otherwise. Recently, meta-analyses showed an increased occurrence of melanoma among patients with PD, and a more recent report involving more than 530,000 patients confirmed that this association remains evident [1,2]. Several overlapping mechanisms have been proposed, including oxidative stress, mitochondrial dysfunction, α-synuclein biology, DNA-damage responses, proteostasis, and inflammatory signaling [3]. Furthermore, recent transcriptomic studies have identified overlapping genes and pathways related to macrophage activity, cell death, metabolism, and immune regulation in PD and melanoma [4,5]. However, the regulatory mechanisms that connect these pathways across neurologic and tumor tissues remain poorly understood.

Immune dysregulation is increasingly recognized as a major component of both diseases. In PD, microglia and other myeloid cells adopt inflammatory states characterized by altered Toll-like receptor (TLR), Nuclear factor kappa-light-chain-enhancer of activated B cells (NF-κB), cytokine, inflammasome, and interferon signaling, while peripheral immune cells may further contribute to neurodegeneration [6,7]. In melanoma, the immune microenvironment contains macrophages, dendritic cells, $CD8^+$ and $CD4^+$ T cells, natural killer cells, and regulatory T cells whose interactions strongly influence tumor progression and therapeutic response [8,9]. Thus, although both disorders display notable immune remodeling, their downstream immune outputs differ substantially. PD is dominated by chronic neuroinflammatory and myeloid responses [10], whereas melanoma frequently exhibits coordinated myeloid, antigen-presenting, and cytotoxic lymphocyte activity [11].

MicroRNAs (miRNAs) may provide a regulatory bridge between these immune environments. Beyond canonical post-transcriptional repression, circulating and extracellular-vesicle-associated miRNAs can participate in intercellular immune signaling. Extracellular miR-574-5p has been shown to bind and activate human TLR8, activating MyD88-dependent cytokine, interferon, and STAT signaling [12], while extracellular-vesicle-associated miR-574-5p has also been linked to TLR7/8 activation [13]. Recent work has therefore highlighted miR-574-5p as a dual-function miRNA capable of both conventional gene regulation and noncanonical innate immune receptor activation [14]. This mechanism is especially relevant to PD and melanoma because the same circulating miRNA could potentially encounter different receptor-expressing immune-cell populations and thereby generate distinct tissue-specific immune responses.

We asked whether available PD and cutaneous-melanoma datasets contain reproducible miRNA associations and convergent immune-expression contexts. We separated newly computed PD serum DESeq2 results and TCGA-SKCM sample-level correlations from source-extracted melanoma, pathway and single-cell findings; assessed cohort and specimen heterogeneity; and audited miRNA–target evidence. The objective was to formulate, not establish, a biologically testable hypothesis about context-dependent extracellular miRNA sensing.

2. Materials and Methods

2.1. Study Design and Data Sources

This exploratory integrative study assessed whether immune-associated molecular profiles in PD and cutaneous melanoma share descriptive features. It was not designed to explain the epidemiological co-occurrence of the diseases or demonstrate causal nature. Data layers were retained separately by specimen, clinical contrast and analysis provenance.

PD miRNA datasets comprised GSE180193 (serum) and two serum-derived extracellular-vesicle (EV) cohorts, GSE269775 (recruited in 2020) and GSE269776 (recruited in 2021). The primary GSE180193 comparison included 61 drug-naïve PD cases and 58 healthy controls recruited in Göttingen; a recruitment-site-adjusted sensitivity analysis also included 19 healthy controls from Bologna. The GSE269775 cohort included 50 PD cases and 50 controls, and GSE269776 included 46 PD cases and 30 controls. Published EV differential-expression estimates were obtained from the investigators' available DESeq2 result tables, whereas the GSE180193 raw serum counts were analyzed in this study. Separate longitudinal rasagiline-treatment cohorts were not included in the PD-versus-control comparison [15,16]. Melanoma datasets were analyzed as distinct clinical and technical evidence sources. GSE150956 comprised two melanoma brain-metastasis plasma cohorts (36 and 24 patients) compared with the same 48 healthy donors [17]. GSE157370 included 47 stage III/IV melanoma patients and 73 controls, with pre-treatment and longitudinal immunotherapy samples; treatment-response associations were distinguished from

disease-control comparisons [18]. GSE143231 included 10 stage-IV melanoma patients and five controls evaluated using different plasma collection tubes, EV preparations, and normalization methods in the same participants [19]. Published differential-expression findings from these melanoma studies were extracted according to their original contrasts; melanoma miRNA datasets were not uniformly reanalyzed from raw counts. Cohort selection and source dependencies are detailed in **Supplementary Table S1**.

2.2. Differential miRNA Analysis and Candidate Selection

GSE180193 raw UMI counts were analyzed in R 4.6.1 using DESeq2 1.52.0 [20]. The primary analysis compared 61 Göttingen drug-naïve PD cases with 58 controls using the model ~ disease_group, DESeq2 median-ratio size-factor normalization, parametric dispersion fitting, and Wald tests with independent filtering. Human miRNAs with nonzero counts were included, and Benjamini–Hochberg FDR < 0.05 defined statistically significant serum discoveries. Sensitivity analyses comprised low-count-filtered Göttingen samples and a mixed-site model (~ recruitment_site + disease_group) including the additional 19 Bologna controls; an unadjusted mixed-site comparison was considered exploratory. Age and sex were not entered as covariates because validated sample-level metadata were insufficient. Analysis code, model outputs, and session information are included in the accompanying reproducibility materials. For a targeted panel of 12 EV miRNAs, log2 fold changes, standard errors, and FDR values were extracted from published GSE269775/GSE269776 results. EV replication required concordant effect directions and FDR < 0.05 in both cohorts; direction-only agreement and opposite-direction findings were recorded separately. A targeted integration inventory comprised the 26 serum discoveries plus five additional EV-panel miRNAs and was used for evidence comparison, not as a transcriptome-wide EV discovery result or a common-FDR set. Melanoma evidence was classified as disease-versus-control, treatment-response-associated, or technical/normalization-dependent. Analyses sharing participants or controls were not counted as independent replications, and nominal *p*-values were distinguished from FDR-adjusted results (**Supplementary Tables S1–S8**).

For GSE180193, the public count matrix contains 165 samples identified by study-internal sample labels. A complete one-to-one crosswalk between these matrix identifiers and GEO GSM accessions could not be independently verified because the available GEO/source metadata does not provide a complete verified correspondence. During the sample audit, five GSM-to-matrix identifier links could be individually verified; the remaining assignments are therefore labeled provisional or unresolved in the accompanying sample manifest rather than treated as confirmed. This limitation prevents reliable participant-level linkage of covariates such as age and sex and restricts participant-level identity auditing; accordingly, the site-matched Göttingen comparison was retained as the primary analysis and the GSE180193 results are interpreted as cohort-level expression associations rather than fully covariate-adjusted participant-level estimates.

2.3. Meta-Analysis and Heterogeneity

For selected miRNAs with complete cohort-level effects and standard errors, the two EV estimates were summarized separately, and a secondary three-cohort inverse-variance random-effects meta-analysis was calculated using the DerSimonian–Laird estimator. Cochran's Q and I^2 quantified between-cohort heterogeneity. Cross-compartment estimates were treated as exploratory summaries rather than homogeneous biological effect sizes. Because EV cohorts may differ in recruitment, pre-analytics and analytic processing, heterogeneity was not attributed to specimen compartment without direct evidence. Leave-one-cohort-out analyses were used for sensitivity. Reported *p* values from distinct serum/EV analyses were not combined into a single global discovery FDR.

Cross-disease *p*-value combination was not performed because GSE150956 MBM comparisons shared healthy controls; GSE157370 included repeated samples and outcome-stratified contrasts; and the GSE143231 tube and normalization comparisons reused participants. The GSE143231 source used a nominal unadjusted significance threshold ($p < 0.05$) together with fold-change filtering for its technical analyses, rather than a uniform cross-miRNA FDR criterion. Candidate ranking therefore considered the clinical contrast, specimen, effect direction, adjustment status, dependence, and orthogonal validation (**Supplementary Tables S2** and **S3**).

2.4. Source-Audited miRNA–Target and Immune-Interaction Evidence

Canonical miRNA–mRNA interactions were curated for three focal miRNAs (nine nominated miR-215-5p pairs, six miR-584-5p pairs, and nine miR-574-5p pairs). Sources were evaluated using miRTarBase 2025 [21] and the primary experimental literature. Each interaction was annotated for miRNA arm, target, species, tissue or cell type, and evidence type, including wild-type/mutant 3′UTR reporter assays, protein measurements, and functional rescue. Direct primary experimental evidence was traceable for ten of 24 evaluated pairs; the other 14 were classified as insufficiently verified and excluded from claims of experimentally established regulation (**Supplementary Tables S9** and **S10**). Extracellular miR-574-5p engagement of human TLR8 was evaluated separately as noncanonical receptor signaling rather than RISC-dependent repression (**Supplementary Table S11**). Immune relevance was assessed from reported gene functions, without performing new version-controlled ImmPort, Reactome, GO, KEGG, or MSigDB enrichment on the small target set.

2.5. Descriptive Target-Direction Compatibility Assessment

Target-direction compatibility was assessed descriptively when a circulating miRNA contrast and an interpretable melanoma tissue-target expression direction were available. Because miRNA and target-mRNA measurements were obtained from different participants and biological compartments, inverse expression was not considered validation of direct regulation; a non-inverse direction does not exclude translational repression. The evaluable comparisons included two of three inverse-compatible targets for miR-215-5p, one of three for miR-584-5p, and one of one for miR-574-5p. These small, dependent sets were summarized descriptively without formal binomial hypothesis testing. Target-level contrasts and evidence limitations are given in **Supplementary Table S12**. The extracellular miR-574-5p–TLR8 interaction was evaluated as receptor engagement and was not subject to an inverse target-expression criterion.

2.6. Provenance-Aware Pathway Evidence Integration

Pathway evidence was extracted from published studies, recording dataset, tissue, comparison, gene-set source, analytical method, and reported statistic. No uniform de novo GSEA was performed across PD and melanoma transcriptomes. In a published combined analysis of substantia nigra cohorts GSE7621, GSE20141, and GSE49036 (45 PD cases and 25 controls), Magalhaes et al. [22] reported KEGG cytokine–cytokine receptor interaction enrichment (NES = 3.5537) and a literature-based type-I interferon signature (NES = 1.686), both with reported $p \leq 0.001$. The melanoma immune-pathway context was drawn from published GSVA, Hallmark, and cell-state analyses involving distinct cohorts and comparisons, including GSE3189, GSE15605, GSE46517, and GSE72056. Only statistics linked to a defined source dataset, gene set, and comparison were presented quantitatively; remaining pathway findings were summarized qualitatively. Type-I interferon and IFNγ programs were considered separately. Given differences in tissues, patient groups, gene-set definitions, and computational procedures, pathway findings were integrated qualitatively rather than combined into cross-disease effect sizes. No pathway-consistency score was interpreted as a direct measure of biological immune activity (**Supplementary Table S13**).

2.7. Source-Aware Cell-Type Assessment and Sample-Level TCGA-SKCM Immune-Module Analysis

PD cell-type context was obtained from published analyses of GSE157783 (five PD donors, six controls) [23] and GSE243639 (15 PD donors, 14 controls) [24]. Published GSE72056 melanoma single-cell findings provided macrophage and pattern-recognition receptor family context [25], without establishing specific TLR8 activation. TCGA-SKCM gene-level RNA-seq expression was obtained through the UCSC Xena TCGA.SKCM.sampleMap release [26]. One tumor sample per participant was retained (n = 470; 104 primary and 366 metastatic). Seven predefined immune-expression modules represented myeloid, dendritic-cell, CD8-effector, NK-cell, type-I interferon, IFNγ response, and chemotaxis programs, calculated from within-gene standardized expression. A separate pan-leukocyte score comprised PTPRC, LCP1, LAPTM5, and CD53 (**Supplementary Tables S14** and **S15**). Sample-level consensus tumor-purity estimates (CPE) from Aran et al. [27] were accessed through TCGAbiolinks Tumor.purity [28] and matched to the expression data using 15-character TCGA sample barcodes. CPE was available for 466 participants (102 primary, 364 metastatic), with alternative LUMP estimates for 457 participants. TLR8–module associations were cal-

culated as Spearman correlations and partial rank correlations, with adjustment for CPE, leukocyte score, and primary/metastatic status. Confidence intervals were calculated using 600 participant-level bootstrap replicates; HC3 robust rank-regression P values were Benjamini–Hochberg-adjusted across the seven modules. LUMP and tumor-subgroup analyses assessed sensitivity (**Supplementary Tables S15–S21**). Correlations were interpreted as expression associations rather than evidence of TLR8 activation.

2.8. Qualitative Immune-Program Evidence Synthesis

Evidence from published pathway and single-cell studies was summarized by individual immune program and tissue context. Myeloid, dendritic-cell, CD8 T-cell, NK-cell, type-I interferon, and IFNγ-related programs were described separately, without imposing an aggregate innate-versus-adaptive polarization index. The published single-cell evidence was used to describe cellular context; no donor-level differential-expression or pseudobulk reanalysis was conducted. Differences in the fractions of recovered cells were not treated as changes in absolute cell abundance. The underlying studies and scope of each analysis are documented in **Supplementary Tables S22** and **S23**.

2.9. Statistical Analysis

Unless otherwise stated, $p < 0.05$ was considered statistically significant. Multiple-testing correction used the Benjamini–Hochberg method, with FDR < 0.05 considered significant. Meta-analysis results are reported as pooled $\log_2$FC estimates with heterogeneity quantified by I^2.

2.10. Ethics Statement

This study used only publicly available datasets and did not involve recruitment of new human participants, collection of biological specimens, or animal experimentation. Therefore, additional institutional ethical approval was not required. Ethical approvals and informed-consent procedures for the original studies are reported in the corresponding source publications.

3. Results

3.1. Primary Serum Discovery and Targeted PD EV Evidence

In the primary Göttingen-only GSE180193 DESeq2 analysis, 26 serum miRNAs met BH-FDR < 0.05 among 61 drug-naïve PD cases and 58 controls (**Figure 1a**; **Supplementary Table S4**). The complete differential-expression results and recruitment-site-adjusted sensitivity results are provided in **Supplementary Tables S4** and **S5**.

Targeted comparison with the two published PD EV cohorts showed heterogeneous replication patterns across 12 selected miRNAs (**Figure 1b**; **Supplementary Table S6**). miR-19b-3p, miR-1537-3p, miR-22-5p, and miR-29b-3p increased significantly in both EV cohorts. miR-584-5p was significant but oppositely directed, whereas miR-574-5p showed opposite directions and attained FDR significance in only one EV cohort. miR-215-5p decreased in both EV cohorts but reached FDR significance in one cohort.

A targeted 31-miRNA inventory combined the 26 serum discoveries with five additional EV-panel candidates for cross-cohort comparison (**Figure 1c**; **Supplementary Table S7**). This inventory documents available effects for selected miRNAs rather than representing a comprehensive EV discovery analysis. miR-215-5p, miR-574-5p, and miR-584-5p were examined in greater detail because they had differing forms of PD and melanoma evidence and biological plausibility.

3.2. Meta-Analysis Identifies One Directionally Consistent Candidate and Pronounced EV Cohort Heterogeneity

miR-215-5p decreased in the primary serum analysis and both EV cohorts, with low heterogeneity in the exploratory cross-compartment meta-analysis (**Figure 1d**; **Table 1**). The two EV cohorts, however, showed opposing effects for miR-574-5p and miR-584-5p, resulting in highly heterogeneous, nonsignificant pooled estimates. The discordance between the two EV cohorts indicates that heterogeneity cannot be explained solely by serum-versus-EV differences (**Supplementary Tables S6** and **S24**).

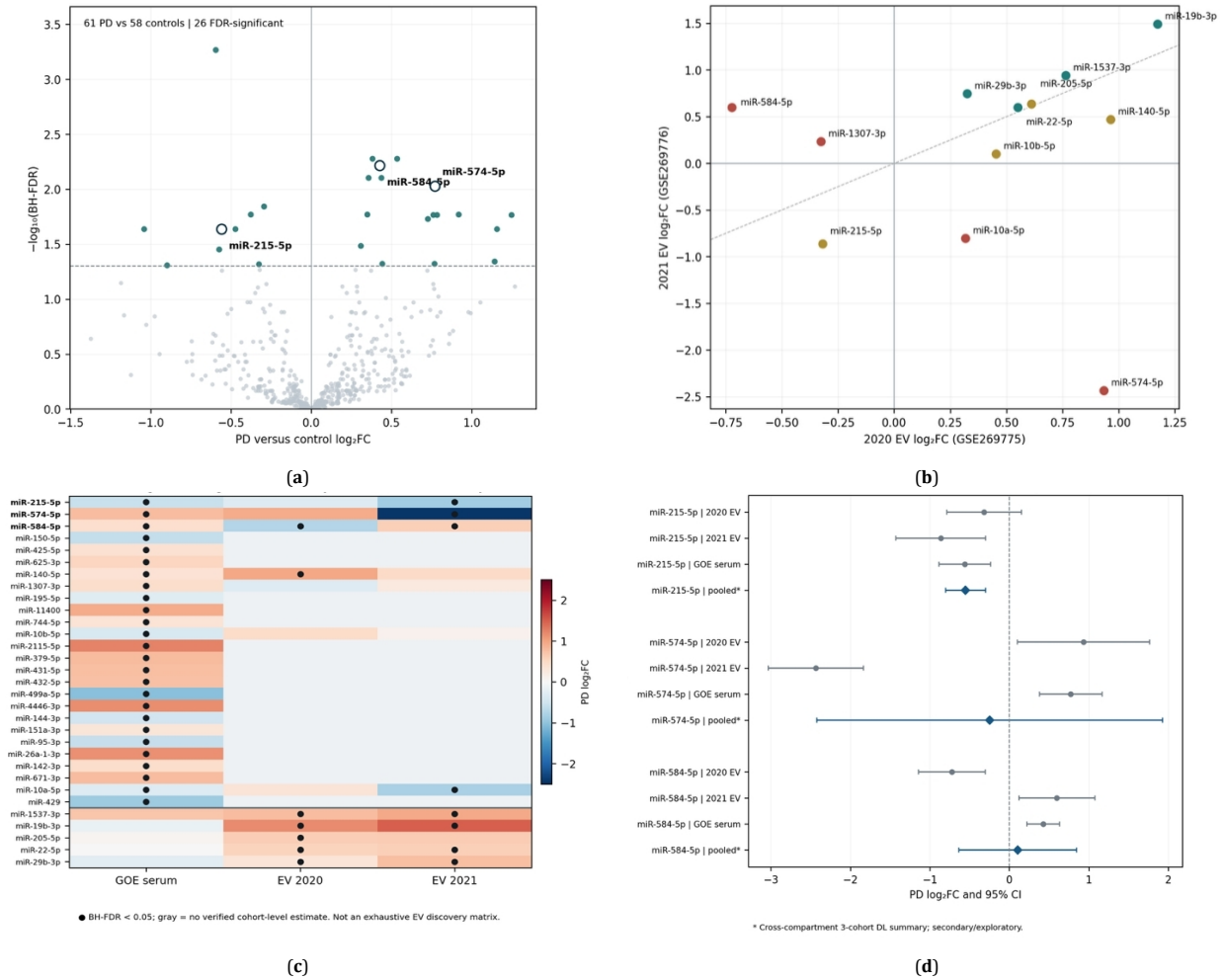

Figure 1. PD serum differential-expression discovery and targeted EV evidence. (**a**) Göttingen-only DESeq2 serum volcano plot shown across the FDR range. (**b**) Published effect estimates for 12 targeted miRNAs in GSE269775 and GSE269776. (**c**) Targeted 31-miRNA integration inventory comprising 26 serum discoveries and five additional EV-panel candidates; dots indicate cohort-specific FDR < 0.05, and missing entries do not imply absence of expression. (**d**) Cohort-specific effects and exploratory three-cohort random-effects estimates for the three focal miRNAs. Cross-compartment pooled estimates are descriptive associations, not mechanistic effect sizes.

The strongest coherent EV-only signal among this targeted panel was miR-19b-3p, which showed increased abundance and individual-cohort FDR significance in both recruitment-year cohorts. It lacked similarly established melanoma disease-associated replication and was retained as a PD-biased candidate rather than a cross-disease marker (**Table 1**). The three-cohort meta-analyses remain secondary descriptive evidence; the site-restricted serum analysis and cohort-specific EV estimates carry the primary inferential interpretation.

Table 1. Cohort-stratified and secondary DerSimonian–Laird random-effects estimates for focal PD miRNAs and miR-19b-3p. Serum effects derive from the independent Göttingen-only DESeq2 analysis; EV effects originate from the original authors' 2020/2021 differential-expression result files.

miRNA	Model	$\log_2$FC	CI Low	CI High	P	I^2 (%)
miR-215-5p	EV-only	−0.567	−1.099	−0.035	0.0367	52.7
miR-215-5p	3-cohort*	−0.552	−0.803	−0.301	1.65×10^{-5}	5.6
miR-574-5p	EV-only	−0.763	−4.065	2.538	0.65	97.6
miR-574-5p	3-cohort*	−0.247	−2.424	1.929	0.824	97.6
miR-584-5p	EV-only	−0.067	−1.362	1.227	0.919	94.0
miR-584-5p	3-cohort*	0.105	−0.637	0.846	0.782	92.2

Table 1. *Cont.*

miRNA	Model	log_2FC	CI Low	CI High	P	I^2 (%)
miR-19b-3p	EV-only	1.303	0.936	1.671	3.74×10^{-12}	0.0
miR-19b-3p	3-cohort*	0.810	−0.337	1.957	0.166	95.7

Note: The 3-cohort* model combines the Göttingen serum cohort with the two PD EV cohorts (GSE269775 and GSE269776) using a DerSimonian–Laird random-effects meta-analysis. Because these cohorts represent different circulating compartments (serum and EV), the pooled estimates should be interpreted as exploratory cross-compartment summaries rather than homogeneous biological effect estimates.

3.3. Melanoma-Source Appraisal Separates Disease Association from Treatment and Technical Evidence

Among melanoma disease-versus-control studies, GSE150956 showed elevated plasma miR-574-5p in two melanoma brain-metastasis comparisons against one shared healthy-control group (**Table 2**; **Supplementary Tables S1** and **S2**). These comparisons provide consistent within-study evidence but are not independent because they share controls. Their direction agrees with the Göttingen PD serum result but not with both PD EV cohorts.

In GSE143231, melanoma EV sequencing suggested reduced miR-215-5p, but the finding was not confirmed by RT-qPCR. Collection-tube and normalization analyses involved the same participants. miR-584-5p was reported in a pretreatment immunotherapy nonresponder-associated signature in GSE157370 and showed normalization-dependent EV evidence in GSE143231. Thus, these observations represent tentative EV, treatment-response-associated, or technical evidence rather than independent melanoma-versus-control replication (**Supplementary Tables S2, S3, S25,** and **S26**).

Table 2. Cross-disease evidence for three circulating miRNAs in PD and melanoma. GSE150956 shares controls, GSE157370 assesses treatment response, and GSE143231 includes repeated technical comparisons; these do not constitute independent disease–control replication.

miRNA	PD Serum DESeq2	PD EV 2020/2021	GSE150956 Disease–Control	GSE157370 Treatment Context	GSE143231 Technical Contrasts
miR-215-5p	Decreased (Göttingen serum)	Decreased in both cohorts (FDR < 0.05 in one)	Not established	Not verified	EV sequencing: decreased; RT-qPCR not confirmed
miR-574-5p	Increased (Göttingen serum)	Opposite directions between EV cohorts	Plasma increased (FC 3.27 and 2.36)	Not verified	Not established
miR-584-5p	Increased (Göttingen serum)	Opposite directions between EV cohorts	Melanoma brain-metastasis plasma: increased	Increased in pretreatment nonresponders	EV finding dependent on geNorm normalization

3.4. Primary-Source Verification Distinguishes Canonical Targets from Extracellular Receptor Engagement

Of 24 evaluated canonical miRNA–target pairs, ten had traceable evidence from primary reporter-based or comparable direct experiments (**Table 3**; **Supplementary Table S9**). These included miR-215-5p with YY1, XIAP, EREG, and HOXB9; miR-584-5p with HDAC1, EIF4E3, WWP1, and MSMO1; and miR-574-5p with FOXN3 and QKI. The remaining pairs did not have sufficient source-level assay documentation to be classified as directly validated. The evidence was generally obtained in models outside matched PD–melanoma patient samples. Separately, miR-574-5p engagement of human TLR8 has been demonstrated experimentally in lupus- and rheumatoid-arthritis-related systems but was not measured in the PD or melanoma cohorts (**Supplementary Table S11**). Target-direction compatibility was descriptive, given the unmatched biological samples and small evaluable sets (**Supplementary Table S12**).

Table 3. Evidence for principal canonical miRNA targets and the separate extracellular miR-574-5p–TLR8 receptor mechanism.

Interaction Class	Verified Examples	Primary Support	Disease Context	Interpretation Limit
Canonical miR-215-5p	YY1, XIAP, EREG, HOXB9	Original WT/MUT reporter or direct assays	Melanoma; bone MSC; colorectal cancer	No matched PD–melanoma patient regulation

Table 3. *Cont.*

Interaction Class	Verified Examples	Primary Support	Disease Context	Interpretation Limit
Canonical miR-584-5p	HDAC1, EIF4E3, WWP1, MSMO1	Original 3′UTR reporter and functional experiments	Medulloblastoma; gastric and breast cancer	Not melanoma-specific regulation
Canonical miR-574-5p	FOXN3, QKI (QKI6 isoform)	Reporter and protein response	Nasopharyngeal/gastric carcinoma	Do not conflate with TLR8 agonism
Noncanonical miR-574-5p	TLR8	Binding assays and receptor-dependent activation	Human autoimmune/arthritis systems	Candidate mechanism only in PD and melanoma
Previously curated (provisional)	14 additional target pairs	Primary assay not established in this study	Not independently established	Exclude from source-verified denominator

3.5. Pathway Analyses Support Qualitative Inflammatory Overlap, Not Matched Disease-Level Enrichment

Published PD substantia nigra GSEA reported enrichment of cytokine–cytokine receptor signaling (NES = 3.5537) and a literature-defined type-I interferon signature (NES = 1.686; both reported $p \leq 0.001$) [22]. Melanoma studies reported TNF/NF-κB-, inflammatory-, JAK–STAT-, and IFNγ-associated states in different clinical and tissue contexts (**Figure 2a**). These observations indicate partially overlapping immune-pathway contexts but do not establish comparable cross-disease enrichment effect sizes. The dataset-specific sources, statistical details where available, and analysis provenance are summarized in **Supplementary Table S13**.

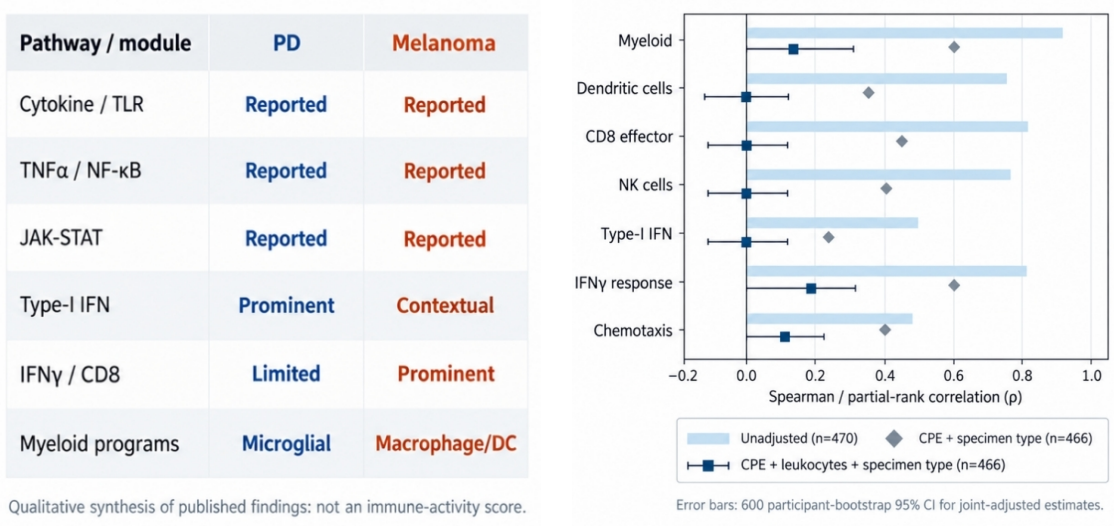

(**a**) (**b**)

Figure 2. Published pathway context and patient-level TLR8 immune-expression associations. (**a**) Qualitative summary of PD and melanoma pathway and cell-state findings, without assigning quantitative immune-activity scores. (**b**) TCGA-SKCM TLR8 associations with seven predefined expression modules. Pale bars show unadjusted Spearman correlations (n = 470); diamonds show CPE- and sample-type-adjusted correlations (n = 466); dark bars show jointly adjusted partial-rank correlations accounting for CPE, pan-leukocyte expression, and tumor sample type (n = 466), with participant-bootstrap 95% CIs.

3.6. TLR8 Tracks Leukocyte Abundance and Retains Selected Residual Immune Associations in TCGA-SKCM

Patient-level TCGA-SKCM analysis confirmed that TLR8 strongly tracks pan-leukocyte expression (Spearman ρ = 0.927) and inversely tracks independently estimated consensus tumor purity (ρ = −0.804; n = 466). Strong unadjusted correlations with all seven immune modules attenuated after joint adjustment for tumor purity, leukocyte-associated expression and primary/metastatic sample type (**Figure 2b**; **Table 4**). A residual IFNγ-response associa-

tion persisted (partial $\rho = 0.252$, 600-bootstrap 95% CI 0.167–0.357), accompanied by a weaker myeloid association ($\rho = 0.208$, 95% CI 0.096–0.325). CD8-effector, dendritic-cell, NK-cell and type-I-IFN estimates were near zero after adjustment. Chemotaxis retained a modest estimate but failed the rank-regression FDR threshold (**Supplementary Table S18**).

LUMP-based purity adjustment supported a similar residual IFNγ and myeloid pattern (**Supplementary Table S19**). Some associations differed between primary and metastatic tumors (**Supplementary Table S20**), although the subgroup results are exploratory and do not constitute formal tests of effect modification. The strong correlation between purity and leukocyte-associated expression indicates that the joint models may be affected by collinearity. Accordingly, the TLR8 results describe composition-sensitive immune co-expression, not receptor activation or direct miR-574-5p–TLR8 signaling. Published single-cell observations provide supplementary cellular context without new donor-aware pseudobulk inference.

Table 4. TLR8–immune-module associations in TCGA-SKCM (n = 470; purity-adjusted n = 466). Models adjust for tumor purity (CPE), specimen type, and, where indicated, leukocyte expression. CIs were estimated using 600 bootstrap replicates; FDR was calculated from HC3 robust rank regression across seven modules.

Module	Unadjusted ρ	CPE-Only ρ	Joint-Adjusted ρ (95% CI)	Joint FDR
Myeloid	0.879	0.605	0.208 (0.096 to 0.325)	0.0012
Dendritic cells	0.752	0.360	−0.010 (−0.124 to 0.097)	0.909
CD8 effector	0.796	0.432	0.006 (−0.097 to 0.118)	0.909
NK cells	0.762	0.405	0.019 (−0.090 to 0.122)	0.909
Type-I IFN	0.485	0.240	−0.009 (−0.103 to 0.090)	0.909
IFNγ response	0.815	0.577	0.252 (0.167 to 0.357)	1.13×10^{-5}
Chemotaxis	0.848	0.565	0.120 (0.003 to 0.237)	0.0877

3.7. Integrated Evidence Supports a Testable, Non-Causal Immune-Context Hypothesis

Across PD and melanoma, the evidence indicates partially overlapping inflammatory-pathway contexts in distinct tissues (**Figure 3a**). Published PD cell-type studies describe microglial and interferon-associated responses, whereas melanoma data show a myeloid-rich immune context with IFNγ-related expression. In TCGA-SKCM, adjusting for tumor purity and leukocyte-associated expression markedly reduced TLR8 correlations with CD8-effector and dendritic-cell modules, showing that unadjusted associations were strongly influenced by cellular composition (**Figure 2b**; **Table 4**).

The experimentally demonstrated extracellular miR-574-5p–human TLR8 interaction in non-PD/non-melanoma immune systems provides a plausible hypothesis for future investigation. Neither the circulating miRNA datasets nor the available brain and tumor expression evidence directly demonstrate ligand delivery or TLR8 activation by miR-574-5p in patients with PD or melanoma. **Figure 3b** illustrates this candidate pathway relationship and the distinct cellular contexts in the two diseases.

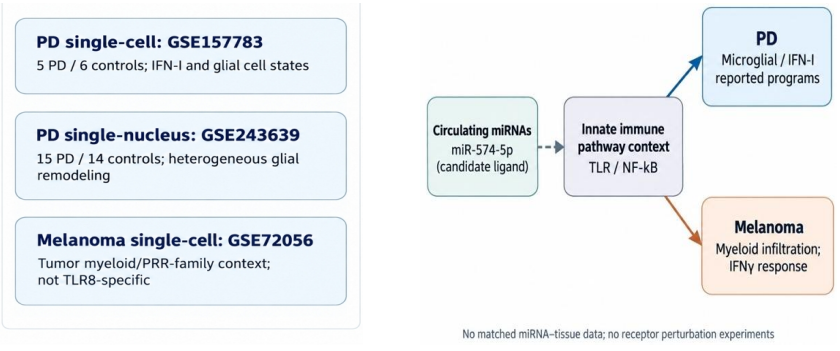

(**a**) (**b**)

Figure 3. Cellular evidence and integrated hypothesis. (**a**) Scope and provenance of published PD and melanoma single-cell observations. (**b**) Conceptual model relating circulating candidate miRNAs to innate immune pathways and disease-associated cellular programs. The dashed arrow indicates the miR-574-5p–TLR8 receptor interaction established in other experimental disease contexts but not directly tested in these patient cohorts.

4. Discussion

This study identifies partially overlapping immune-expression contexts in PD and melanoma while distinguishing statistical miRNA associations from experimentally established mechanisms in other systems. In TCGA-SKCM, TLR8 expression correlated strongly with leukocyte-associated gene expression and inversely with estimated tumor purity. Joint adjustment for tumor purity, leukocyte score, and sample type substantially attenuated the CD8-effector, dendritic-cell, NK-cell, and type-I interferon associations. Residual IFNγ-response and weaker myeloid associations persisted, but remained co-expression findings rather than direct evidence of TLR8 signaling.

miR-215-5p demonstrated relatively consistent PD-associated downregulation, although its melanoma EV sequencing signal was not confirmed by RT-qPCR. By contrast, miR-574-5p is supported as a human TLR8 ligand in experimental immune-disease systems but displayed heterogeneous effects between the two PD EV cohorts. This discordance cannot be assigned to EV-versus-serum compartment differences alone. Selective EV cargo packaging, sample collection, separation, carrier heterogeneity, and normalization procedures can influence circulating-miRNA measurements [29–31]. Biological source, recruitment, and preanalytic differences remain alternative explanations for the observed heterogeneity.

Extracellular miR-574-5p–TLR8 receptor engagement differs mechanistically from canonical 3′-UTR target repression. Wang and colleagues demonstrated human TLR8 engagement with downstream MyD88/NF-κB and interferon-associated responses in a lupus-related experimental context [12]. Hegewald and colleagues reported TLR7/8-dependent responses to extracellular miR-574-5p in rheumatoid-arthritis-related systems [13], and a mechanistic review distinguishes these receptor effects from intracellular target regulation [14]. Separately, a mouse MPTP study implicated TLR7/8 pathways in glial and neuronal responses [32]. Critically, the strongest direct evidence for extracellular miR-574-5p engagement of human TLR8 comes from lupus- and rheumatoid-arthritis-related experimental systems, not from PD or melanoma. None of the PD or melanoma patient datasets analyzed here measured miR-574-5p binding to TLR8, receptor activation after miRNA exposure, or a TLR8-dependent functional response. Thus, these external experiments provide the mechanistic precedent for a candidate hypothesis but do not constitute evidence that miR-574-5p–TLR8 signaling occurs in the patients analyzed here (**Supplementary Table S11**).

In PD, the published GSE157783 study described cell-type-specific type-I interferon activity [23], and GSE243639 documented glial and immune-cell remodeling [24]. Human brain-region studies also report region- and cell-type-dependent interferon responses [33]. Together with work on systemic neuroimmune mechanisms [6,7], these findings provide a plausible inflammatory context but do not establish TLR8 activation by circulating miRNA or a universal increase in absolute microglial abundance. No donor-aware single-cell differential-expression analysis was generated within the present study.

Even within PD, type-I interferon cannot be assigned a single beneficial or detrimental direction. Neuronal IFNβ/IFNAR dysfunction has been linked experimentally to mitochondrial stress, α-synuclein accumulation, and PD-related cognitive pathology [22], whereas other studies document inflammatory and interferon-associated programs in glial states [23,24,33]. These findings underscore the importance of cell type, brain region and disease context, consistent with broader reviews of convergent and divergent PD mechanisms [6,34]. Our data do not support a claim of universally increased type-I interferon signaling across the PD brain.

In melanoma, the patient-level analysis demonstrates the importance of immune-cell admixture in bulk transcriptomic interpretation. Controlling for tumor purity, pan-leukocyte expression, and sample type reduced most TLR8–immune-module associations substantially; IFNγ-response and a weaker myeloid module retained residual correlations. These observations are compatible with the known cellular heterogeneity of melanoma [35,36], published observational TLR7/8–immune-marker relationships [37], and chemokine-dependent immune organization [38]. They do not identify a TLR8-specific signaling state or determine whether any particular extracellular miRNA is responsible.

In melanoma, an IFNγ-associated expression pattern should not be equated automatically with effective antitumor immunity. Clinical-response studies associate IFNγ responsiveness with immune-checkpoint blockade benefit [39], but sustained IFNγ can also constrain intratumoral stem-like T-cell persistence [40] and participate in melanoma resistance programs [41]. Spatial analyses further emphasize the organization of T cells and dendritic

cells during successful treatment responses [42]. The present TCGA module results cannot resolve these functional or spatial states, particularly because many unadjusted correlations reflect differences in leukocyte abundance.

Supporting miRNAs provide experimentally testable precedents, not additional validated shared PD–melanoma biomarkers. EV-associated miR-19b-3p can repress SOCS1 and promote macrophage inflammatory responses in a kidney-injury model [43], but its relevance to PD myeloid signaling has not been demonstrated here. miR-150 has been implicated in CD8 T-cell differentiation through FOXO1 and c-Myb regulatory pathways [44,45]. Because equivalent melanoma miRNA-expression comparisons and matched target responses were not established, neither pathway was promoted as a causal cross-disease link.

Evidence for other immune-relevant miRNAs remains context-dependent. miR-140-5p targeted the TLR4 3′UTR in an oxidized-LDL-treated THP-1 model [46], but that result does not directly extend to PD or melanoma. Candidate interactions involving miR-29 and lymphocyte-associated regulators are summarized in **Supplementary Table S11**. In the absence of matched circulating-miRNA and tissue-target measurements, a miRNA expression change cannot be used to infer repression of a specified brain or melanoma gene.

miR-215-5p remains a comparatively consistent PD expression candidate, but its canonical targets require independent appraisal. A melanoma-cell study reported a miR-215-5p/YY1 interaction within a circHIPK3-associated regulatory model [47], whereas XIAP, EREG and HOXB9 target evidence derives from other cell contexts (**Supplementary Table S9**). Because no matched patient-level circulating miR-215-5p and melanoma target-expression data were available, directionally compatible observations are descriptive and are not considered target validation (**Table 3**; **Supplementary Table S12**).

A further limitation is that TLR/NF-κB, cytokine and interferon signaling are not specific to the PD–melanoma pair. Related innate programs occur across neurodegenerative disorders [6,34] and multiple tumor microenvironments [35,36]. The epidemiological association between PD and melanoma may also involve α-synuclein biology, oxidative stress, mitochondrial and lysosomal dysfunction, pigmentation-associated pathways and cell-survival programs [3, 34]. Therefore, the shared pathway patterns described here represent a candidate layer of biological overlap, not a comprehensive explanation for why the diseases co-occur.

This analysis has several limitations. The datasets differ in circulating-miRNA carriers, sequencing platforms, patient populations, specimen processing, tissues, and clinical contrasts, with no matched miRNA and tissue-target measurements. Pathway evidence was obtained from heterogeneous published GSEA/GSVA and related analyses rather than a uniform de novo enrichment pipeline. Primary experimental assays could be traced for ten of 24 candidate canonical target pairs, and most were conducted outside PD or melanoma. Tumor-purity and leukocyte-score adjustments reduce, but cannot eliminate, the influence of cell composition or unmeasured confounders on TCGA co-expression. Single-cell observations were derived from source publications without a new donor-aware pseudobulk reanalysis. For GSE180193, the incomplete independently verified GSM-to-matrix-ID crosswalk additionally limits participant-level identity auditing and linkage to individual covariates; this is why the serum findings are interpreted as site-matched cohort-level associations rather than fully covariate-adjusted participant-level estimates. Therefore, the evidence supports an exploratory shared-pathway hypothesis, not direct ligand-mediated communication or a causal explanation for the epidemiological association (**Supplementary Tables S9–S13, S22** and **S23**).

Accordingly, the principal value of this integration is the generation of a specific, falsifiable hypothesis rather than evidence that the proposed mechanism already operates in PD or melanoma patients. These limitations define the most important experimental next steps. A decisive test would require matched extracellular-RNA and tissue immune profiling in the same individuals, with separation of free, protein-bound, and EV-associated miR-574-5p. In PD-relevant systems, human iPSC-derived microglia or primary monocyte-derived myeloid cells could be exposed to physiologically relevant miR-574-5p-containing fractions, followed by TLR8 inhibition or genetic disruption and measurement of MyD88, NF-κB, STAT1, cytokine, and IFN-I responses. In melanoma, analogous experiments in macrophage/dendritic-cell cultures and tumor–immune co-cultures could test whether miR-574-5p/TLR8 activation alters antigen presentation, chemokine production, and recruitment or activation of CD8 T cells. Spatial transcriptomics combined with small-RNA profiling would be especially informative because recent melanoma studies indicate that immune response depends not only on the presence of immune populations but also on their spatial organization [8,42].

5. Conclusions

In conclusion, the integrated PD and melanoma evidence indicates partially shared inflammatory-pathway contexts, not demonstrated miRNA-mediated communication. In TCGA-SKCM, most TLR8–immune-module associations attenuated after joint adjustment for tumor purity and leukocyte-associated expression, although residual IFNγ-response and weaker myeloid associations remained. miR-215-5p is a relatively consistent PD candidate, whereas miR-574-5p displays substantial cross-cohort heterogeneity despite established extracellular human TLR8 ligand activity in other disease settings. Together, these findings generate a specific, tissue- and cell-context-dependent, falsifiable hypothesis involving extracellular miR-574-5p and TLR8, but provide no direct evidence that this ligand–receptor interaction occurs in PD or melanoma patients or explains their epidemiological association.

Supplementary Materials

Supplementary data supporting this study are available at https://ojs.ukscip.com/uploads/2/asset-file/2026/11/asset-file_eaacb757e00a47236ca6ae42128aba0f.xlsx.

Author Contributions

A.L.E. and H.P. shared first authorship. Conceptualization, F.M.S.; methodology, F.M.S.; validation, F.M.S. and A.A.; formal analysis, A.L.E. and H.P.; investigation, A.L.E. and H.P.; data curation, A.L.E. and H.P.; writing—original draft preparation, A.L.E. and H.P.; writing—review and editing, F.M.S. and A.A.; visualization, A.L.E. and H.P.; supervision, F.M.S.; project administration, F.M.S. All authors have read and agreed to the published version of the manuscript.

Funding

This work received no external funding.

Institutional Review Board Statement

This study used only publicly available datasets and did not involve recruitment of new human participants, collection of biological specimens, or animal experimentation. Therefore, additional institutional ethical approval was not required. Ethical approvals and informed-consent procedures for the original studies are reported in the corresponding source publications.

Informed Consent Statement

Not applicable.

Data Availability Statement

The publicly available miRNA datasets were obtained from NCBI GEO (GSE180193, GSE269775, GSE269776, GSE150956, GSE157370, and GSE143231) (https://www.ncbi.nlm.nih.gov/geo/). Published single-cell analyses used GSE157783, GSE243639, and GSE72056; the PD pathway source included GSE7621, GSE20141, and GSE49036. TCGA-SKCM expression was obtained through UCSC Xena (https://xenabrowser.net/), and tumor-purity estimates were matched from the TCGAbiolinks Tumor.purity resource. Dataset- and analysis-level provenance is documented in **Supplementary Tables S1, S13, S21,** and **S26**. The accompanying reproducibility archive includes the GSE180193 sample manifest with GSM-mapping verification status and explicitly marked unresolved fields, the DESeq2 analysis code, model outputs and session information, TCGA-SKCM immune-module calculation and statistical-analysis scripts with module definitions, and the source-audited target-verification evidence tables; no new primary sequencing data were generated.

Acknowledgments

The authors gratefully acknowledge the investigators and participants of the original studies whose publicly available datasets were used in this research. We also acknowledge the National Center for Biotechnology Informa-

tion Gene Expression Omnibus (NCBI-GEO), The Cancer Genome Atlas (TCGA), and the NCI Genomic Data Commons for providing open access to the molecular and transcriptomic data that enabled this integrative analysis.

Conflicts of Interest

The authors declare no conflict of interest.

AI Use Statement

During the preparation of this work, the authors used ChatGPT and TrinkaAI for grammar checking and academic language polishing. The authors subsequently reviewed and edited the content as necessary and take full responsibility for the final content of the published article.

References

1. Mehdiyeva, A.; Kaasinen, V.; Heervä, E.; et al. Impact of Parkinson's disease diagnosis validity on the association with cancer: A systematic review and meta-analysis. *Parkinsonism Relat. Disord.* **2025**, *135*, 107846. [CrossRef]
2. Huang, P.; Yang, X.-D.; Chen, S.-D.; et al. The association between Parkinson's disease and melanoma: A systematic review and meta-analysis. *Transl. Neurodegener.* **2015**, *4*, 21.
3. Aiello, J.; Zamarato, R.; Moscheni, C.; et al. Revisiting the alpha-synuclein paradox in melanoma-Parkinson's disease connection: More than a tale of two cell fates. *Cell. Mol. Life Sci.* **2025**, *83*, 7. [CrossRef]
4. Wang, Q.; Duan, Y.; Xu, Y.; et al. Linking Parkinson's disease and melanoma: The impact of copper-driven cuproptosis and related mechanisms. *NPJ Parkinson's Dis.* **2025**, *11*, 74. [CrossRef]
5. Zhang, L.; Li, D.; Zheng, X.; et al. Exploring the underlying molecular connections: A bioinformatics approach to link melanoma and Parkinson's disease. *Front. Genet.* **2025**, *16*, 1526018. [CrossRef]
6. Weiner, H.L. Immune mechanisms and shared immune targets in neurodegenerative diseases. *Nat. Rev. Neurol.* **2025**, *21*, 67–85. [CrossRef]
7. Mohan, M.; Mannan, A.; Singh, T.G. Parkinson's disease: Exploring the systemic immune mechanisms through molecular investigations. *Inflammopharmacology* **2025**, *33*, 3679–3699. [CrossRef]
8. Magrill, J.; Moldoveanu, D.; Gu, J.; et al. Mapping the single cell spatial immune landscapes of the melanoma microenvironment. *Clin. Exp. Metastasis* **2024**, *41*, 301–312. [CrossRef]
9. Zilberg, C.; Ferguson, A.L.; Lyons, J.G.; et al. The tumor immune microenvironment in primary cutaneous melanoma. *Arch. Dermatol. Res.* **2025**, *317*, 273. [CrossRef]
10. Song, Z.; Li, W.; Han, Y.; et al. Association of immune cell traits with Parkinson's disease: A Mendelian randomization study. *Front. Aging Neurosci.* **2024**, *16*, 1340110. [CrossRef]
11. Tucci, M.; Passarelli, A.; Mannavola, F.; et al. Immune system evasion as hallmark of melanoma progression: The role of dendritic cells. *Front. Oncol.* **2019**, *9*, 1148. [CrossRef]
12. Wang, T.; Song, D.; Li, X.; et al. MiR-574-5p activates human TLR8 to promote autoimmune signaling and lupus. *Cell Commun. Signal.* **2024**, *22*, 220. [CrossRef]
13. Hegewald, A.B.; Breitwieser, K.; Ottinger, S.M.; et al. Extracellular miR-574-5p induces osteoclast differentiation via TLR 7/8 in rheumatoid arthritis. *Front. Immunol.* **2020**, *11*, 585282. [CrossRef]
14. Yang, J.Y. miR-574-5p in epigenetic regulation and Toll-like receptor signaling. *Cell Commun. Signal.* **2024**, *22*, 567. [CrossRef]
15. Zago, E.; Dal Molin, A.; Dimitri, G.M.; et al. Early downregulation of hsa-miR-144-3p in serum from drug-naïve Parkinson's disease patients. *Sci. Rep.* **2022**, *12*, 1330. [CrossRef]
16. Yu, Z.; Saiki, S.; Shiina, K.; et al. Comprehensive data for studying serum exosome microRNA transcriptome in Parkinson's disease patients. *Sci. Data* **2024**, *11*, 1128. [CrossRef]
17. Bustos, M.A.; Tran, K.D.; Rahimzadeh, N.; et al. Integrated assessment of circulating cell-free microRNA signatures in plasma of patients with melanoma brain metastasis. *Cancers* **2020**, *12*, 1692. [CrossRef]
18. Bustos, M.A.; Gross, R.; Rahimzadeh, N.; et al. A pilot study comparing the efficacy of lactate dehydrogenase levels versus circulating cell-free microRNAs in monitoring responses to checkpoint inhibitor immunotherapy in metastatic melanoma patients. *Cancers* **2020**, *12*, 3361. [CrossRef]
19. Schneegans, S.; Lück, L.; Besler, K.; et al. Pre-analytical factors affecting the establishment of a single tube assay for multiparameter liquid biopsy detection in melanoma patients. *Mol. Oncol.* **2020**, *14*, 1001–1015.

20. Love, M.I.; Huber, W.; Anders, S. Moderated estimation of fold change and dispersion for RNA-seq data with DESeq2. *Genome Biol.* **2014**, *15*, 550. [CrossRef]
21. Cui, S.; Yu, S.; Huang, H.-Y.; et al. miRTarBase 2025: Updates to the collection of experimentally validated microRNA-target interactions. *Nucleic Acids Res.* **2025**, *53*, D147–D156. [CrossRef]
22. Magalhaes, J.; Tresse, E.; Ejlerskov, P.; et al. PIAS2-mediated blockade of IFN-β signaling: A basis for sporadic Parkinson disease dementia. *Mol. Psychiatry* **2021**, *26*, 6083–6099. [CrossRef]
23. Quan, P.; Li, X.; Si, Y.; et al. Single cell analysis reveals the roles and regulatory mechanisms of type-I interferons in Parkinson's disease. *Cell Commun. Signal.* **2024**, *22*, 212. [CrossRef]
24. Martirosyan, A.; Ansari, R.; Pestana, F.; et al. Unravelling cell type-specific responses to Parkinson's disease at single cell resolution. *Mol. Neurodegener.* **2024**, *19*, 7. [CrossRef]
25. Tirosh, I.; Izar, B.; Prakadan, S.M.; et al. Dissecting the multicellular ecosystem of metastatic melanoma by single-cell RNA-seq. *Science* **2016**, *352*, 189–196. [CrossRef]
26. Goldman, M.J.; Craft, B.; Hastie, M.; et al. Visualizing and interpreting cancer genomics data via the Xena platform. *Nat. Biotechnol.* **2020**, *38*, 675–678. [CrossRef]
27. Aran, D.; Sirota, M.; Butte, A.J. Systematic pan-cancer analysis of tumour purity. *Nat. Commun.* **2015**, *6*, 8971. [CrossRef]
28. Colaprico, A.; Silva, T.C.; Olsen, C.; et al. TCGAbiolinks: An R/Bioconductor package for integrative analysis of TCGA data. *Nucleic Acids Res.* **2016**, *44*, e71. [CrossRef]
29. Dixson, A.C.; Dawson, T.R.; Di Vizio, D.; et al. Context-specific regulation of extracellular vesicle biogenesis and cargo selection. *Nat. Rev. Mol. Cell Biol.* **2023**, *24*, 454–476. [CrossRef]
30. Tran, V.; de Oliveira-Jr, G.P.; Chidester, S.; et al. Choice of blood collection methods influences extracellular vesicles counts and miRNA profiling. *J. Extracell. Biol.* **2024**, *3*, e70008. [CrossRef]
31. van Niel, G.; Carter, D.R.F.; Clayton, A.; et al. Challenges and directions in studying cell-cell communication by extracellular vesicles. *Nat. Rev. Mol. Cell Biol.* **2022**, *23*, 369–382. [CrossRef]
32. Campolo, M.; Filippone, A.; Biondo, C.; et al. TLR7/8 in the pathogenesis of Parkinson's disease. *Int. J. Mol. Sci.* **2020**, *21*, 9384. [CrossRef]
33. Garza, R.; Adami, A.; Thiruvalluvan, A.; et al. Activation of transposable elements is linked to a region- and cell type-specific interferon response in Parkinson's disease. *Sci. Adv.* **2026**, *12*, aed2952. [CrossRef]
34. Coukos, R.; Krainc, D. Key genes and convergent pathogenic mechanisms in Parkinson disease. *Nat. Rev. Neurosci.* **2024**, *25*, 393–413. [CrossRef]
35. Heras-Murillo, I.; Adán-Barrientos, I.; Galán, M.; et al. Dendritic cells as orchestrators of anticancer immunity and immunotherapy. *Nat. Rev. Clin. Oncol.* **2024**, *21*, 257–277. [CrossRef]
36. Kalaora, S.; Nagler, A.; Wargo, J.A.; et al. Mechanisms of immune activation and regulation: Lessons from melanoma. *Nat. Rev. Cancer* **2022**, *22*, 195–207. [CrossRef]
37. Zhang, M.; Yan, Z.; Wang, J.; et al. Toll-like receptors 7 and 8 expression correlates with the expression of immune biomarkers and positively predicts the clinical outcome of patients with melanoma. *Onco Targets Ther.* **2017**, *10*, 4339–4346. [CrossRef]
38. Mempel, T.R.; Lill, J.K.; Altenburger, L.M. How chemokines organize the tumour microenvironment. *Nat. Rev. Cancer* **2024**, *24*, 28–50. [CrossRef]
39. Grasso, C.S.; Tsoi, J.; Onyshchenko, M.; et al. Conserved interferon-γ signaling drives clinical response to immune checkpoint blockade therapy in melanoma. *Cancer Cell* **2020**, *38*, 500–515. [CrossRef]
40. Mazet, J.M.; Mahale, J.N.; Tong, O.; et al. IFN*γ* signaling in cytotoxic T cells restricts anti-tumor responses by inhibiting the maintenance and diversity of intra-tumoral stem-like T cells. *Nat. Commun.* **2023**, *14*, 321. [CrossRef]
41. Lim, S.Y.; Shklovskaya, E.; Lee, J.H.; et al. The molecular and functional landscape of resistance to immune checkpoint blockade in melanoma. *Nat. Commun.* **2023**, *14*, 1516. [CrossRef]
42. Di Pietro, A.; Au, L.; Crock, P.; et al. Tumor-resident T cells and dendritic cells form an in situ archetype during immunotherapy response in melanoma. *Nat. Commun.* **2026**, *17*, 7445. [CrossRef]
43. Lv, L.-L.; Feng, Y.; Wu, M.; et al. Exosomal miRNA-19b-3p of tubular epithelial cells promotes M1 macrophage activation in kidney injury. *Cell Death Differ.* **2020**, *27*, 210–226. [CrossRef]
44. Ban, Y.H.; Oh, S.-C.; Seo, S.-H.; et al. miR-150-mediated Foxo1 regulation programs CD8+ T cell differentiation. *Cell Rep.* **2017**, *20*, 2598–2611. [CrossRef]
45. Chen, Z.; Stelekati, E.; Kurachi, M.; et al. miR-150 regulates memory CD8 T cell differentiation via c-Myb. *Cell Rep.* **2017**, *20*, 2584–2597. [CrossRef]

46. Liu, H.; Mao, Z.; Zhu, J.; et al. MiR-140-5p inhibits oxidized low-density lipoprotein-induced oxidative stress and cell apoptosis via targeting toll-like receptor 4. *Gene Ther.* **2021**, *28*, 413–421. [CrossRef]
47. Zhu, X.; Sun, J. CircHIPK3 regulates melanoma cell behaviors by binding with miR-215–5p to upregulate YY1. *Mol. Cell. Probes* **2020**, *53*, 101644. [CrossRef]



Copyright © 2026 by the author(s). Published by UK Scientific Publishing Limited. This is an open access article under the Creative Commons Attribution (CC BY) license (https://creativecommons.org/licenses/by/4.0/).

Publisher's Note: The views, opinions, and information presented in all publications are the sole responsibility of the respective authors and contributors, and do not necessarily reflect the views of UK Scientific Publishing Limited and/or its editors. UK Scientific Publishing Limited and/or its editors hereby disclaim any liability for any harm or damage to individuals or property arising from the implementation of ideas, methods, instructions, or products mentioned in the content.